Applied Catalysis B: Environmental 229 (2018) 204–210

Contents lists available at ScienceDirect

Applied Catalysis B: Environmental

journal homepage: www.elsevier.com/locate/apcatb

Multiaspect insight into synergetic modification of carbon nitride with halide salt and water vapor

Wenting Wu[a], Wenming Xu[a], Xianghui An[a], Lizhuo Wang[a], Jing Zhang[b], Zhongtao Li[a,*], Mingbo Wu[a,*]

[a] State Key Laboratory of Heavy Oil Processing, College of Chemical Engineering, China University of Petroleum (East China), Qingdao, 266580, PR China
[b] State Key Laboratory of Safety and Control for Chemicals, SINOPEC Research Institute of Safety Engineering, Qingdao, 266071, PR China

ARTICLE INFO

Keywords:
Carbon nitride
Photocatalysis
Halide salt
Synergistic effect

ABSTRACT

Carbon nitride shows great potential in photocatalysis, to some extent, due to its insolubility and high thermal, chemical and optical stability. However, it always brings great difficulties for its surface modification and hinders the photocatalysis development. Traditional salt without melting condition is hard for the direct modification of carbon nitride. Herein, pristine carbon nitride (CN) was further modified through the synergetic modification of halide salts (NaCl and KCl) and water vapor. For the obtained product (Na-K-4h), it was carefully studied from three points: the appearance and morphology, the change of chemical structure and composition, and the chemical analysis of its by-products. These researches reveal that H_2O could be divided into H and OH. H helps the halide away from halide salt, while the left OH replaces NH groups and help K and Na chelate with CN. This method could also be applied to other salt mixture system (such as NaCl/KI, NaCl/KBr). In this work, Na-K-4h was further applied in photocatalystic H_2 evolution (PHE). Based on this synergistic effect, Na-K-4h show about 27-fold PHE activity higher than CN.

1. Introduction

Carbon-based materials are particularly attractive due to environment and sustainability concerns [1,2]. Carbon nitride, as a carbon-based material and a representative organic semiconductor photocatalyst, has recently attracted widespread attention due to its excellent performance in H_2 evolution [3–6], organic pollutant degradation [7–9], CO_2 reduction [10–12] and artificial photosynthesis [13,14]. In addition, it could be facilely obtained through the thermal polymerization of inexpensive materials (urea, melamine, dicyanamide and others), together with its insolubility and the high thermal, chemical and optical stability. However, these excellent properties, at the same time, bring lots of difficulties in modifying carbon nitride itself for further enhancing the photocatalysis ability. Series of modification methods have been developed including morphology design [15,16], elemental doping [17,18], copolymerization [19], and construction of g-C_3N_4-based semiconductor composites [20,21]. However, most of these methods were processed with the initial materials or active intermediates, and there are few reports about the modification of the stable products under mild condition.

Halide salt was considered as suitable candidates for the material modification. In the 1960s, Sundermeyer et al. showed that lots of organic chemistry could be carried out in molten halide salts [22,23]. In 2008, carbon nitride was successfully synthesized from dicyandiamide by using molten halide salts [24]. And then graphitic carbon nitride possessing crystalline structure were obtained with halide salts (e.g. KCl/LiCl, KBr/LiBr, LiCl·H_2O/KCl/NaCl) [25–28]. But for most of halide salt, their salt melting temperatures are higher than the thermal stability temperature of carbon nitride which can destroy its main structure and hinder its modification. Actually, there are some unreacted functionalized groups such as NH and C≡N on the surface of carbon nitride, and the addition of halide salt, to some extent, may break the heptazine core [29]. In other words, these provide efficient active sites to react with other organic, inorganic compounds, H_2O or metals.

Inspired by this idea, the synergistic reaction of carbon nitride, H_2O and halide salts (NaCl, KCl) at 550 °C was designed. Via the synergistic reaction, the pristine carbon nitride grows out OH, C≡N and metal dopants (Na, K). Benefiting from the synergistic effect of NaCl, KCl and H_2O, final product shows excellent photocatalytic hydrogen evolution (PHE) activity owing to the large surface area, extended visible light absorption, the efficient separation ability of photo-generated electron and hole and the synergistic effect of Na^+ and K^+. Furthermore, it was extended to other halide salts (such as NaCl/KI, NaCl/KBr) to confirm their synergistic effect with water and carbon nitride. This method

* Corresponding authors.
E-mail addresses: liztao@upc.edu.cn (Z. Li), wumb@upc.edu.cn (M. Wu).

https://doi.org/10.1016/j.apcatb.2018.02.027
Received 31 August 2017; Received in revised form 6 January 2018; Accepted 11 February 2018
Available online 12 February 2018
0926-3373/

could provide a facile modification for broader organic semiconductors.

2. Experimental

2.1. Materials

Dicyandiamide (99%), KCl (99%) and NaCl (99%) were purchased from Aladdin Industrial Corporation. They were used without further purification.

2.2. Preparation of the photocatalysts

Bulk g-C_3N_4 was prepared by heating 10 g of dicyandiamide up to 550 °C with a ramp rate of 2.3 °C/min and kept for 4 h in a tube furnace covered by an aluminum foil under a N_2 atmosphere. The sample obtained was denoted as CN. After that, 600 mg of the CN sample was ground fully with a mixture of KCl (600 mg) and NaCl (600 mg). Then, the mixture was heated to 550 °C for 4 h with a ramp rate of 5 °C /min in the tube furnace without aluminum foil under a flowing N_2 with water vapor. After cooled to room temperature, the product was further ground and ultrasonically cleaned in deionized water for 20 min. Finally, it was washed with deionized water and centrifuged for several times and collected by filtration followed by drying at 60 °C. The sample obtained was denoted as Na-K-4h.

For comparison, crude CN was further heated to 550 °C for 4h under the same conditions, which was referred to as CN-4h. 600 mg of CN sample was ground with NaCl (1200 mg) and then heated to 550 °C for 4 h. The product was denoted as Na-4h. 600mg of CN sample was ground with KCl (1200 mg) and then heated to 550 °C for 3 h and 4 h. The products were denoted as K-3h and K-4h.

2.3. Characterization

The structure and morphology of the samples were characterized by X-ray diffraction (XRD) (X'Pert PRO MPD, Holland), scanning electron microscopy (SEM) (Hitachi SU8010, Japan). The functional groups in the samples were characterized by Fourier transform infrared spectrometry (FT-IR) (Thermo Nicolet NEXUS670, USA). Further evidence for the composition of the product was inferred from X-ray photoelectron spectroscopy (XPS), using a Kratos AXIS Ultra spectrometer equipped with a prereduction chamber. Elemental analysis was detected by an Elementar Vario EL III instrument (Elementar, Germany). The UV-vis diffused reflectance spectra was obtained for the dry-pressed disk samples using a Scan UV-vis spectrophotometer (UV–vis DRS UV-2700, Shimadzu, Japan) equipped with an integrating sphere assembly, using BaSO4 as a reflectance sample. Nitrogen adsorption-desorption isotherms were obtained on a nitrogen adsorption apparatus (Micromeritics ASAP 2020M) with all samples degassed at 423 K for 12 h prior to measurements. Time-resolved fluorescence decay spectra was performed by an Edinburgh FLS980 spectrophotometer with the excitation wavelength at 375 nm and the emission wavelength at 450 nm. Photoluminescence spectra (PL) was measured on a fluorospectrophotometer (F97pro, Lengguang Tech, China).

2.4. Photocatalytic hydrogen activity test

Photocatalytic hydrogen evolution was performed as follows. 2 mg of the catalyst powder was dispersed in 2 mL aqueous solution containing 10 vol.% triethanolamine scavengers flushed with Ar gas. 2 wt. % Pt was loaded on the surface of the photocatalyst as a cocatalyst using an in-situ photodeposition method with K_2PtCl_6. The solution was then irradiated with a 300 W xenon lamp equipped with a 420 nm cutoff filter at room temperature. The concentration of hydrogen gas in a headspace was quantified by a Shimadzu GC-2014 gas chromatograph (Ar carrier, a capillary column with molecular sieves 5A) equipped with a thermal conductivity detector.

The apparent quantum yield (AQY) for the photocatalytic hydrogen evolution (PHE) was determined by replacing the 420 nm cutoff filter with a 400 nm band-pass filter. The irradiation area was 1.4 cm^2. The total intensity irradiation was measured using a radiometer (TES-1333R solar power meter) by averaging 5 times in the irradiation area. The average intensity was 19.2 mW cm^{-2}. The AQY was calculated as

$$\mathrm{AQE} = \frac{N_e}{N_p} \times 100\% = \frac{2MN_A hc}{SPt\lambda} \times 100\%$$

Where N_e is the amount of reaction electrons, N_p is the amount of incident photons, M is the amount of H_2 molecules, N_A is Avogadro's constant, h is the Planck constant, c is the speed of light, S is the irradiation area, P is the intensity of the irradiation, t is the photoreaction time, and λ is the wavelength of the incident light.

3. Results and discussion

3.1. Feasibility analysis

Based on the thermosgravimetric-differential scanning calorimetry analysis (TG-DSC) of the CN (Fig. S1a) and its mixture with NaCl, KCl, H_2O (Fig. S1b), there is obvious endothermal peak in the temperature range 520–570 °C, and the weight of the mixture decreased rapidly at about 550 °C (peak value). It indicates that the reaction of NaCl, KCl, H_2O and CN is an endothermic reaction and it could happen during this temperature range. Based on the thermal analysis of the mixture of NaCl and KCl (the mixture of 50 wt.% NaCl and 50 wt.% KCl), their melting point is at about 660 °C with obvious endothermal behavior (Fig. S1c) which is in accordance with the phase diagram (Fig. S1d). The mixture of NaCl and KCl hardly played as fuse salts to etch parent CN in this reaction. It indicates that H_2O plays an important role in this reaction. In order to confirm it, the dry NaCl, KCl and CN were sealed in a 7 mm inner diameter quartz tube and then heated under 550 °C for comparison (Fig. S2). Its color and FT-IR spectra have almost no obvious change. Therefore, the water vapor is favorable for the efficient reaction of carbon nitride and halide salts.

In order to study the synergy of carbon nitride with halide salts and water vapor, the pristine carbon nitride (CN) mixed with halide salts (NaCl, KCl or their mixture) with a certain ratio. Then the mixture was reheated at 550 °C under the flowing N_2 and water vapor atmosphere with different post-treatment time (Fig. 1). The final product was obtained after washing with deionized water to remove the soluble salt(s), and they were named Na-4h, K-3h, Na-K-4h, wherein the number represents the reheating hours at 550 °C. In addition, CN mixed with KCl was reheated for 3 h rather than 4 h, just because prolonging the reheated time to 4 h easily results in 'carbonization' of carbon nitride. In order to compare the effect of halide salt, CN was also reheated for 4 h without halide salt, and CN-4h was obtained.

3.2. Characterization of the samples

The appearance and morphology were firstly studied for the synergistic reaction. After post-treatment, these materials show various colors providing an obvious evidence for the synergistic reaction of CN, H_2O and halide salt(s) (Figs. S3 and Figure 2a inset). Na-4h shows bright yellow color, which is similar to parent CN. After post-treatment with KCl, the color changes to brown with an enhancing absorption ability. Interestingly, the synergistic effect of NaCl, KCl and H_2O leads to the yellow-green color of Na-K-4h, which may be attributed to the structure exfoliation [30]. Furthermore, the sample is hardly obtained under air atmosphere, which indicates CN was fully decomposed owing to the air oxidation (Fig. S4). UV–vis DRS (Fig. 2a) were used to carefully study the visible light absorption ability of these materials. Benefiting from the synergistic effect of NaCl and KCl, Na-K-4h has a progressive redshift in the visible absorption edge which is stronger than K-

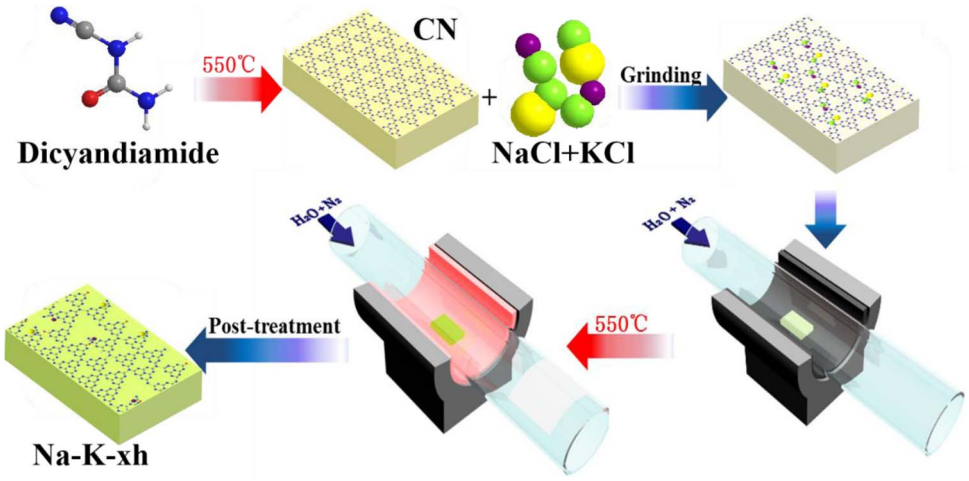

Fig. 1. The schematic diagram of the synergistic reaction of CN, H_2O and halide salt(s).

3h and Na-4h. It benefits for enhancing visible absorption ability of photocatalysis. Furthermore, bandgaps determined from the transformed Kubelka–Munk function progressively narrowed from 2.78 eV for CN to 2.60 eV for Na-K-4h (Fig. S5). These results exhibit the synergistic reaction of NaCl and KCl is beneficial for enhancing visible absorption ability than single NaCl or KCl.

In addition, this synergistic effect brings the improvement of morphology for Na-K-4h. It has obvious regular 'fingers' with the distance of ~1.6 nm (Fig. 2b), and others (e.g. CN, K-3h, Na-4h and CN-4h) show no crystal lattice (Fig. S6), which may be attributed to the synergistic effect of NaCl and KCl. Based on the nitrogen adsorption − desorption isotherms (Fig. S7a), Na-K-4h has a typical type IV isotherm featuring a pronounced H2-type hysteresis loop in the 0.4–0.9 relative pressure (P/P_0) region, while CN-4h has a H3-type hysteresis loop. In contrast, no obvious hysteresis loop was observed for CN, Na-4h and K-3h. The pore size distribution determined by the BJH method indicates that the mean pore size of Na-K-4h is centered at approximately 6 nm, whereas K-3h and Na-4h do not show the obvious pore structure, which could also be ascribed to the synergistic reaction of the mixture of NaCl and KCl (Fig. S7b). As the result of Brunauer-Emmett-Teller (BET) analysis, parent CN has a surface area of 8.1 m^2/g. Na-4h and K-3h show 10.0 m^2/g and 4.3 m^2/g respectively (Table S2). These results are in accordance with morphological characteristics (the smaller the volume, the larger the surface area). Due to the synergistic reaction of NaCl and KCl, it enhances the surface area of Na-K-4h to 39.8 m^2/g. The lattice structure and large surface area of Na-K-4h could improve the electron transfer ability and provide more active sites for the photocatalysis.

The change of chemical structure and composition was then studied to insight into the synergetic effect. After post-treatment with H_2O and halide salt, hydroxyl groups were introduced into Na-K-4h, which was confirmed by electron spin resonance (ESR) analysis. Generally, ·OH may be generated via direct hole oxidation of surface hydroxyl groups or indirect hole oxidation of OH^- from H_2O [29]. The OH group under Ar atmosphere can also turn to ·OH with obvious DMPO–·OH adducts signal (1:2:2:1 quartet). As shown in Fig. 3a, signals corresponding to DMPO–·OH (a = 14.9 G) were observed for Na-K-4h under visible-light irradiation for 12 min, while no relative signal from CN is observed (Fig. S8a). To exclude the possibility that ·OH is derived from the OH- in the H_2O ($H_2O \leftrightarrow H^+ + OH^-$), ·H signals corresponding to DMPO-H was further measured under the Ar atmosphere. But little DMPO–H signals (1:1:2:1:2:1:2:1:1) [31] was observed for Na-K-4h which indicates the ·OH originates from the surface of Na-K-4 instead of H_2O (Fig. S8b).

As the introduction of OH, the content of N—H (NH, NH_2) groups decreased. In FT-IR, all samples including CN and CN-4h show the same s-triazine breathing mode peaks at 810 cm^{-1} and N—C=N heterorings stretching vibration peaks at 900–1800 cm^{-1} respectively (Fig. 3b) [32]. It indicates that their typical heptazine core (tri-s-triazine ring) structures were not changed obviously. However, the materials with the post-treatment have obvious stretching vibrations of O—H at about 3440 cm^{-1} in FT-IR, while there is little N—H (NH, NH_2) stretch at about 3150 cm^{-1} compared with CN and CN-4h. Moreover, there appear extra bands at about 2182 cm^{-1} compared with CN, indicating the existence of C≡N groups [33]. All these results imply that the CN

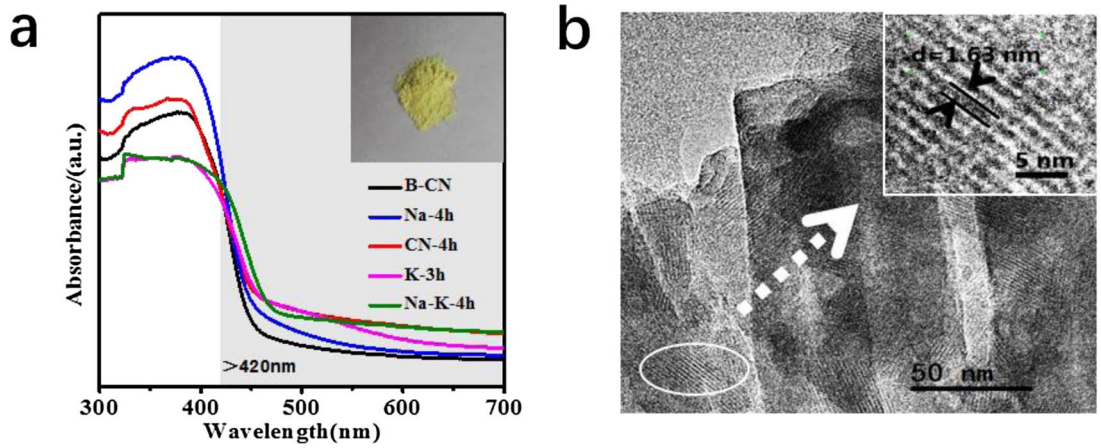

Fig. 2. (a) UV–vis diffuse reflectance spectra of the corresponding samples and the photograph (inset) of Na-K-4h, (b) TEM images of Na-K-4h.

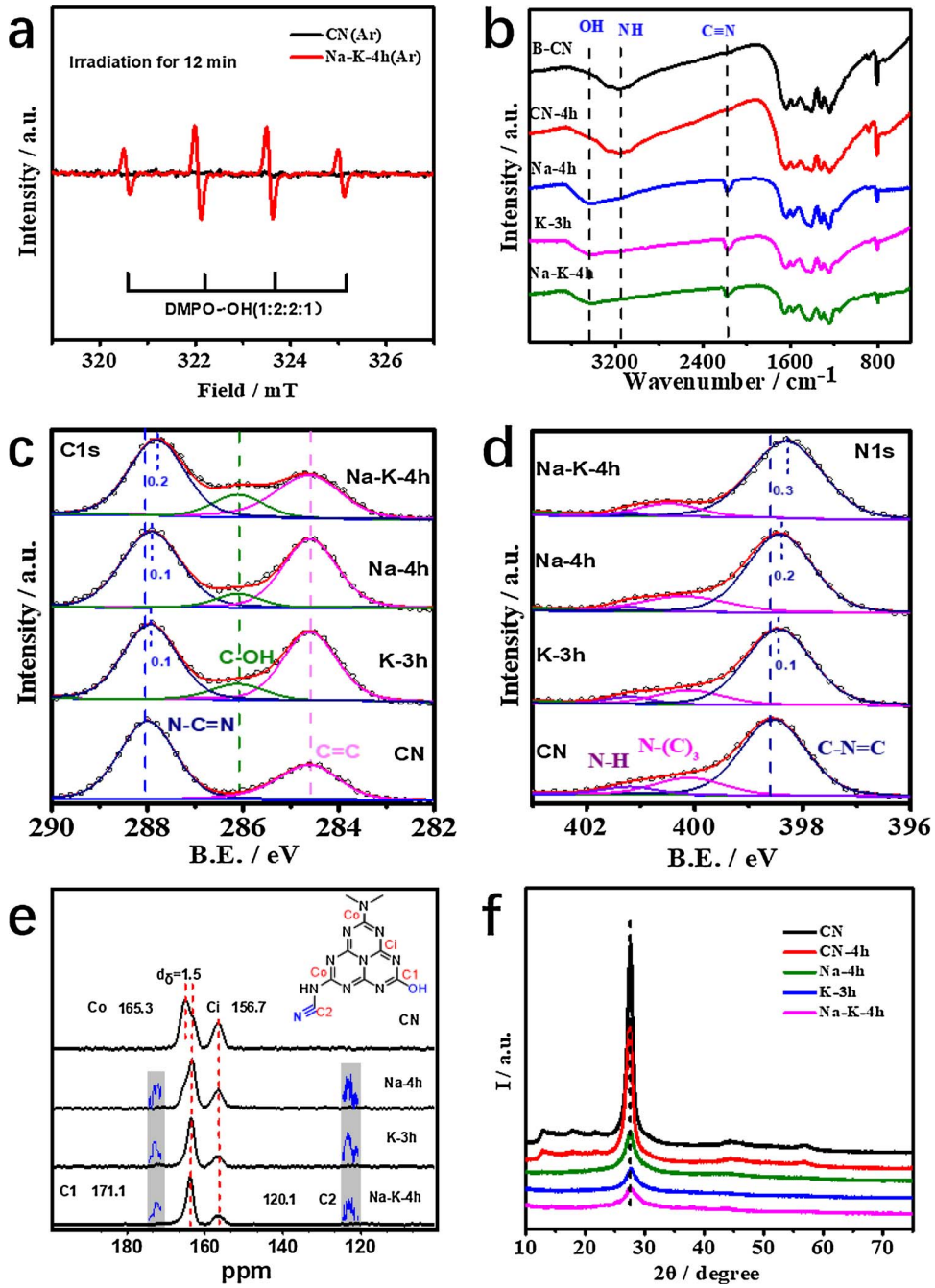

Fig. 3. (a) ESR singnal of Na-K-4h and CN under visible-light irradiation for 12 min Ar atmosphere. (b) FT-IR spectra of samples. The high resolution spectra of C1s (c) and N1s (d) of samples, (e) Solid-state ^{13}C MAS NMR spectra of these samples and proposed structure diagram (inside), the amplified spectra could be seen in Fig. S10. (f) XRD spectra of samples.

framework partly changed upon metal doping; some triazine rings were broken and sp^2 C—N bonds were transformed into C≡N triple bonds [34]. However, the triazine rings still remain, indicating that the major structure changes are only partial.

To some extent, XPS could quantitatively measure this surface change. All products after the synergistic reaction exhibit obvious sp^2 C (C—OH) peaks at 286.1 eV (Fig. 3c) [35]. Compared with CN, Na-K-4h show a 78% decrease on the peak area ratio of N—H (401.2 eV) to N═C—N (about 398.3 eV) in XPS N1s spectra (Fig. 3d, Table S2 and Fig. S9) [36]. The decrease of K-3h and Na-4h could come to 77% and 65% respectively. These results are in accordance to the FT-IR results above. In addition, there is a 77.5% decrease for Na-K-4h on the peak area ratio of N-$(C)_3$ (400.5 eV) to N═C—N (about 398.3 eV) than that of CN, indicating that N-$(C)_3$ structure had been partly destroyed. These results indicate that the N-$(C)_3$ may be broken during the synergic reaction with NaCl, KCl and water vapor, and C—N—H of CN may be further replaced by C—OH.

The solid-state magic angle spinning NMR was also performed to gain more insights into the local structure of the modified materials relative to the CN. The typical ^{13}C NMR in all samples have two distinct peaks (Ci and Co) derived from the heptazine core (Figs. 3e and S10). Compared with CN (Co at 165.3 ppm), Co in Na-4h, K-3h and Na-K-4h shows chemical shifts to high magnetic field (163.8 ppm), while the corresponding Ci has no obvious shift (156.7 ppm) [37]. This shift change may be ascribed to the introduction of OH with relative high electron density. And OH may be close to Co or share the same π conjugation. In addition, there are new peaks (C1, about 171.1 ppm) derived from Co (about 163.8 ppm), further indicating that OH may be

replaced NH_2 at the Co position and formed C1 [32]. In addition, the corresponding ^{13}C signal of C2 (C≡N groups) is also observed at 120.1 ppm consistent with previous reports [38]. Thus, the samples after synergistic effect with halide salts and water mainly possess the typical tri-s-triazine core structure and change a little due to the existence of OH and C≡N.

These OH, C≡N and metal dopants also suppressed the intensity of (002) diffraction peak. CN shows the typical crystal structure of graphitic carbon nitride with the distinct peak at 27.6° (*d*-value, 0.323 nm) and 12.8° (*d*-value, 0.691 nm), which were attributed to (002) interlayer-stacking reflection and (001) in-plane structural packing motif from tri-s-triazine cores respectively (Fig. 3f) [39]. After the introduction of OH, C≡N, and metal dopants (Na^+, K^+), Na-4h, K-3h and Na-K-4h show obvious change with the disappearance of (001) in-plane structural packing motif and the obvious weakened intensity of the (002) interlayer-stacking reflection, which are very similar to those of metal-doped g-C_3N_4 reported [34]. In addition, no significant diffraction peaks of any other phases (NaCl or KCl) or impurities can be detected, which indicates the samples were washed completely and did not form a new crystal structure. Considering relative low surface areas of these products (8.1 m^2/g for CN, 10.0 m^2/g for Na-4h, 4.3 m^2/g for K-3h and 39.8 m^2/g for Na-K-4h; Table S1), the very low (002) diffraction peaks were not derived from the reduced length of interlayer periodicity, but mainly attributed to the introduction of OH, C≡N and metal dopants, which restrain the diffraction of X-rays. The disappearance of (001) diffraction peak indicates the destroying of in-plane structural packing motif owing to the introduction of groups mentioned above.

In addition, Na^+ and/or K^+ were successfully introduced into the materials with the help of water vapor. The XPS survey spectra and corresponding high-resolution XPS spectra show the existence of Na^+ or (and) K^+ but little signal of Cl^-, which directly indicates the chemical reaction of CN and halide salt (NaCl and KCl) (Fig. S11). Furthermore, compared with bonding energy of NaCl and KCl, binding energies of Na^+ and K^+ show negative shifts about 0.33 eV and 0.25 eV in Na-K-4h respectively. It indicates these metal dopants coordinate with lower electronegative groups from carbon nitride rather than Cl (Fig. S11c and d). Note that the bonding energy of all elements was all rectified based on impurity carbon (284.6 eV) [40]. The surface and bulk metal content of corresponding products was summarized in the Table S3. Based on XPS results, the surface metal content of resultant products exhibits 3.2 atm.% Na for Na-4h, 3.7 atm.% K for K-3h, and 2.7 atm.% Na and 3.0 atm.% K for Na-K-4h. The surface metal contents are so high that they were not neglected and could affect the surface properties to some extent. The bulk Na or K content was detected by inductively coupled plasma atomic emission spectroscopy (ICP-AES), which was consistent with XPS results. Surprisingly, the total bulk metal amount of Na-K-4h can reach 8.8 wt.%. Therefore, K and Na are important components in the structure of Na-K-4h, which could also be confirmed from the SEM mapping images (Fig. S12).

3.3. By-products discussion

From the chemical point of view, the by-products were studied to indirect confirm the synergetic reaction. Generally, the NH in the CN is difficult for further polymerization at its synthetic temperature (550 °C) owing the stereospecific blockade. However, great drop of NH content means the NH may react with other reagents. To confirm the conclusion, the by-products (white solid) at the end of the quartz tube was analyzed (Fig. 4). It was shown that the white solid was completely dissolved in deionized water (Fig. 4a and b). Subsequently, $AgNO_3$ solution (0.1 mol/L) was dripped into the aqueous solution of white solid. White floc quickly appeared (Fig. 4c) indicating that there was a large amount of Cl^-. The existence of NH_4^- could be confirmed by Nessler reagent (0.09 mol/L HgIK and 2.5 mol/L KOH). After adding the Nessler reagent, the solution of white solid white became reddish brown (Fig. 4d), suggesting the existence of NH_4^-. Based on the XRD spectra of white solid, there is few miscellaneous peaks and the crystal diffraction peaks are consistent with that of NH_4Cl crystal (JCPDS-ICDD 00-007-0007) demonstrating that the white sample is the NH_4Cl crystal (Fig. 4e). These results further explain the disappearance of NH groups and Cl^- and the residual Na^+ and K^+ left in Na-K-4h mentioned above. It could also indirectly confirm that H of H_2O participates into the formation of NH_4Cl, and OH of H_2O replaces NH (Fig. 4).

3.4. Photocatalytic activity of the samples

Due to the synergistic modification for carbon nitride, the electron-hole recombination got significantly improved. Firstly, it was proved by steady and time-resolved photoluminescence (PL) spectra. Generally, the lower the PL intensity, the lower the recombination rate of photo-induced electron–hole pairs [41]. As shown in steady PL spectra (Fig. 5a inset), CN shows the highest PL intensity among these materials. After interaction with NaCl or KCl, the PL intensity of Na-4h and K-3h shows greatly decreased. Interestingly, after the synergistic effect of NaCl and KCl, the PL of Na-K-4h was sharply quenched and almost disappeared. In the time-resolved PL spectra (Fig. 5a), the lifetime of Na-K-4h is only 1.5 ns, which is much shorter than Na-4h (2.4 ns), K-3h (4.7 ns) and CN (9.0 ns). The quenching of the emission intensity and its lifetime implies that the relaxation of Na-K-4h excitons occurs via nonradiative paths, presumably by charge transfer of electrons and holes with high mobility to new localized states [42]. These results indicate that the synergistic effect of NaCl and KCl greatly suppresses the electron-hole pair recombination.

To further analyze the generation of unpaired electrons and holes in the photocatalyst, as-prepared samples were measured by ESR spectroscopy. As shown in Fig. 5b, the tensor parameter (*g*) is 2.0021, which originates from the unpaired electrons in the conduction band of typical CN semiconductor [43,44]. In comparison with CN, Na-K-4h shows a much stronger signal for unpaired electrons exposed to visible light, indicating the improved efficiency of electron-hole separation after salts modification. Furthermore, Fig. 5c shows the transient photocurrent responses via five on-off cycles of CN, CN-4h, Na-4h, K-3h and Na-K-4h electrodes. As the result, the visible irradiated photocurrent density of Na-K-4h is about 13 times higher than that of CN. The higher photocurrent of Na-K-4h suggests the enhanced separation efficiency of the photogenerated electrons and holes [45].

The VB XPS was employed to determine the electronic structure (Fig. S13). Compared with CN (1.71 eV), the VB of Na-K-4h (1.52 eV) shows a negative shift, which is also more negative than others (–0.09 eV for Na-4h, –0.07 eV for K-3h). Combined with the bandgap obtained from the Kubelka–Munk function (Fig. S5) [40], their conduction bands (CB) were also calculated and shown in Fig. S14. Interestingly, the bandgaps are reduced after the reaction (2.78 eV for CN, 2.76 eV for Na-4h, 2.64 eV for K-3h, 2.60 eV for Na-K-4h). This enhanced optical property is expected to be more beneficial for photocatalytic hydrogen evolution, since more visible photons might be harvested to run photocatalytic reactions. Otherwise, the tunable CB and VB position will be beneficial to modify CN for different application demands.

The photocatalytic activities of the samples were investigated by H_2 evolution from water containing triethanolamine as a sacrificial electron donor under visible light irradiation ($\lambda > 420$ nm). Based on the excellent properties mentioned above, Na-K-4h shows excellent photocatalytic hydrogen evolution (PHE) activity (7.02 μmol, Fig. 5d). In addition, the PHE activity of Na-4h (0.19 μmol) is lower than that of K-3h (0.84 μmol) and even lower than that of CN (0.26 μmol), although Na-4h owns more excellent separation efficiency of photoexcited carriers and higher surface area (10.0 m^2/g for Na-4h, 4.3 m^2/g for K-3h). These results indicate the excellent separation efficiency of photo-excited carriers, surface area and defects (OH, C≡N) could improve photocatalytic activity to some extent, but the synergistic effect of Na^+

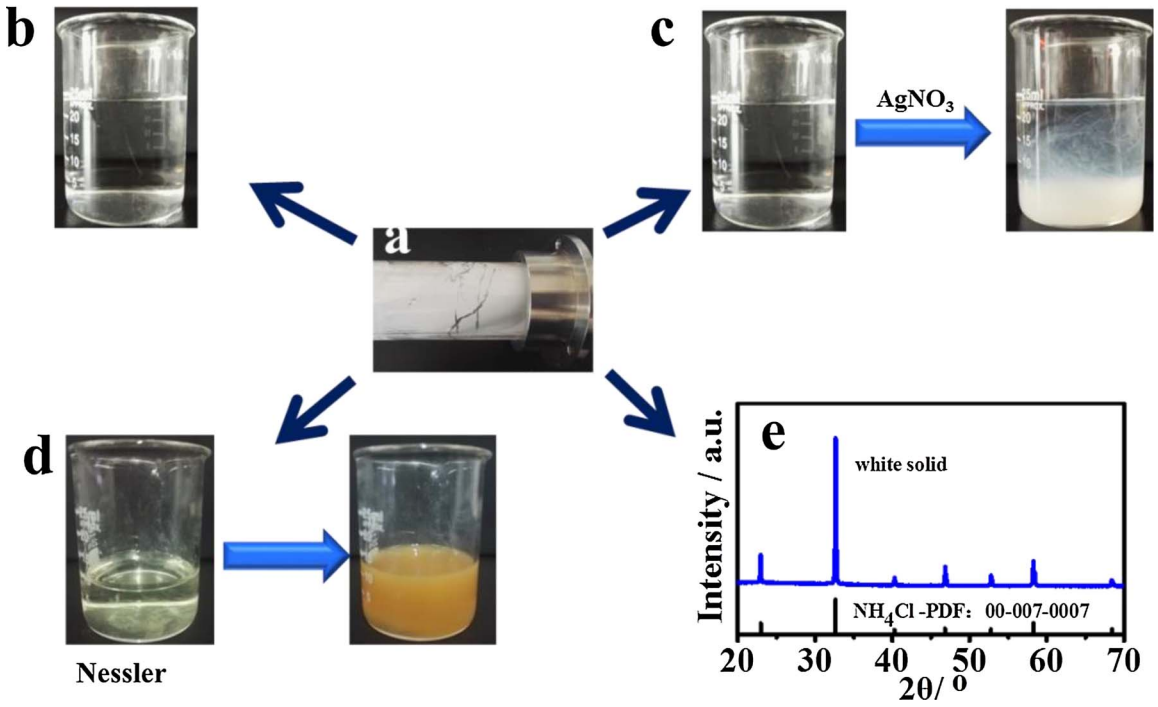

Fig. 4. The photograph of white solid in the quartz tube wall (a) and its aqueous solution (b). The color change of white solid solution after adding $AgNO_3$ solution (c). The color change of Nessler after adding white solid (d). XRD pattern of the white solid (e).

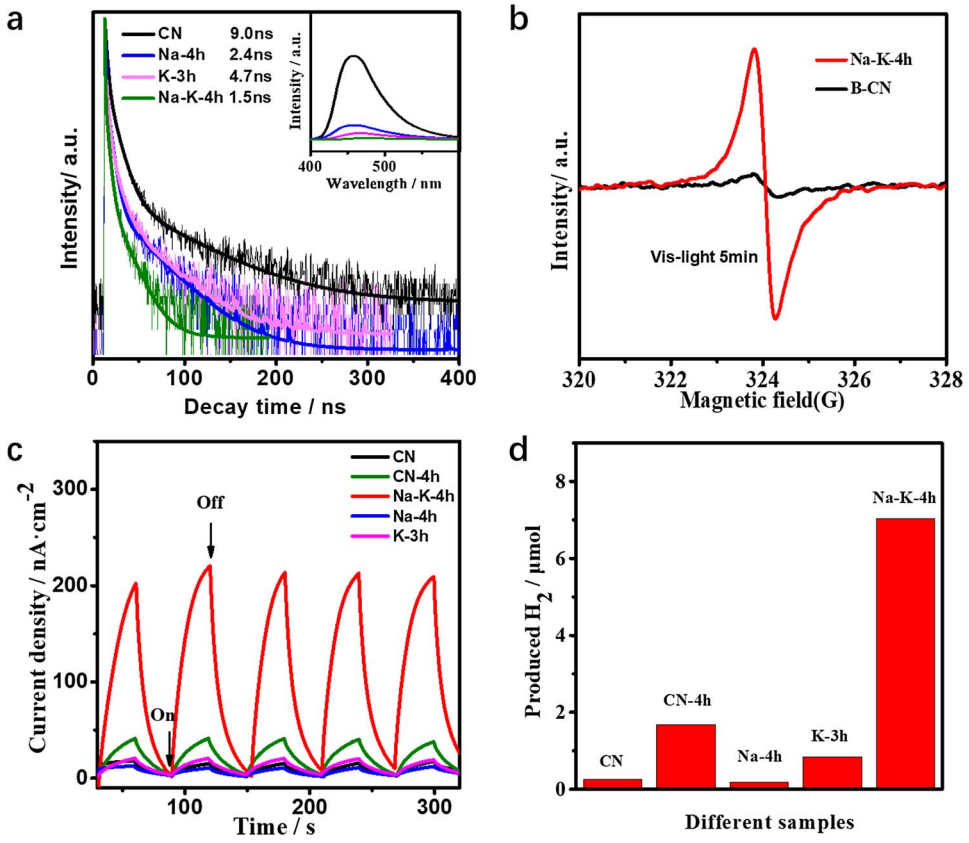

Fig. 5. (a) Time-resolved photoluminescence spectra and photoluminescence spectra of the samples under 350 nm excitation (inset). (b) ESR spectroscopy and (c) Photocurrent response of CN and Na-K-4h. (d) PHE activities of samples in the first four hours.

and K^+ is also more important. As a result of synergistic effect of NaCl and KCl, Na-K-4h shows about 27 times higher PHE activity than CN (37 times than Na-4h, 8.4 times than K-3h, 4.2 times than CN-4h). Because of the excellent properties of Na-K-4h, the cycle stability test of Na-K-4h was further tested and the results were shown in Fig. S15. After the first photocatalysis cycle completed, a distinct decrease in PHE occurs and then negligible change of PHE in subsequent cycle testing. The results indicate the easy shedding of the modification metal ions

and Pt with violent agitation in PHE, which is probably attributed to the weak interactions between Pt nanoparticles or metal ions and ultrathin nanosheets. Despite the photocatalyst is not very stable for reaction system requiring agitation, Na-K-4h still keep about 10 times higher PHE activity after 16 h than CN.

3.5. Other halide salts expansion

Notably, the synergistic reaction of H_2O, NaCl and KCl with CN can be expanded to other halide salts mixture such as NaCl/KI and NaCl/KBr. The color of the as-prepared NaCl-KBr-2h (Fig. S16a) and NaCl-KI-2h (Fig. S16b) was much heavier than that of CN (NaCl-KBr-2h: yellow; NaCl-KI-2h: yellow-green), indicating the enhancement of absorbability for visible light. It was further confirmed by the FT-IR spectra that the strong OH and C≡N stretch vibration peaks of NaCl-KBr-2h and NaCl-KI-2h are similar to that of Na-K-4h (Fig. S16c).

4. Conclusion

In summary, we explored a synergistic reaction to modify carbon nitride with halide salts (e.g. NaCl and KCl) and H_2O at a relatively mild condition. The occurrence of the synergistic reaction mainly relies on breaking chemical bond of CN and introducing of H_2O, K and Na, which has been carefully proved from three points of views. Base on the synergistic modification of CN, the surface areas, visible light absorption ability and efficient separation ability of photogenerated eletron and hole were greatly improved. Via the synergistic effect of NaCl, KCl and water vapor, Na-K-4h show about 27-fold PHE activity with respect to its pristine counterpart. Besides, other halide salts (such as KI, KBr) were also involved to confirm this method. The synergistic reaction will bring more surprises in the future while resultant products may have more excellent photocatalytic properties for practical application.

Acknowledgments

This work was financially supported by NSFC (51672309, 21302224, 51172285, 51372277 and 21503279), Shandong Provincial Key Research Program (2015GSF121017), Project of Science and Technology Program for Basic Research of Qingdao (14-2-4-47-jch) and the Fundamental Research Funds for Central Universities (18CX07009A < GN4 > , < GN4 > 15CX05010A, 15CX08005A and 15CX05013A).

Appendix A. Supplementary data

Supplementary material related to this article can be found, in the online version, at doi:https://doi.org/10.1016/j.apcatb.2018.02.027.

References

[1] X. Fan, C. Yu, J. Yang, Z. Ling, C. Hu, M. Zhang, J. Qiu, Adv. Energy Mater. 5 (2015) 1401761.
[2] Y. Chen, J. Zhang, Acc. Chem. Res. 47 (2014) 2273–2281.
[3] W. Wu, J. Zhang, W. Fan, Z.s. Li, L. Wang, X. Li, Y. Wang, R. Wang, J. Zheng, M. Wu, H. Zeng, ACS Catal. 6 (2016) 3365–3371.
[4] Q. Xiang, J. Yu, M. Jaroniec, Chem. Soc. Rev. 41 (2012) 782–796.
[5] L. Ge, C. Han, Appl. Catal. B: Environ. 117 (2012) 268–274.
[6] X. Li, J. Yu, M. Jaroniec, Chem. Soc. Rev. 45 (2016) 2603–2636.
[7] J. Zhang, X. An, N. Lin, W. Wu, L. Wang, Z. Li, R. Wang, Y. Wang, J. Liu, M. Wu, Carbon 100 (2016) 450–455.
[8] C. Han, L. Ge, C. Chen, Y. Li, X. Xiao, Y. Zhang, L. Guo, Appl. Catal. B: Environ. 147 (2014) 546–553.
[9] Y. Ishida, L. Chabanne, M. Antonietti, M. Shalom, Langmuir 30 (2014) 447–451.
[10] J. Mao, T. Peng, X. Zhang, K. Li, L. Ye, L. Zan, Catal. Sci. Technol. 3 (2013) 1253–1260.
[11] S. Bai, X. Wang, C. Hu, M. Xie, J. Jiang, Y. Xiong, Chem. Commun. 50 (2014) 6094–6097.
[12] S. Liu, D. Li, H. Sun, H.M. Ang, M.O. Tadé, S. Wang, J. Mater. Sci. Technol. 468 (2016) 176–182.
[13] X. Chen, J. Zhang, X. Fu, M. Antonietti, X. Wang, J. Am. Chem. Soc. 131 (2009) 11658–11659.
[14] F. Su, S.C. Mathew, G. Lipner, X. Fu, M. Antonietti, S. Blechert, X. Wang, J. Am. Chem. Soc. 132 (2010) 16299–16301.
[15] Y.S. Jun, E.Z. Lee, X. Wang, W.H. Hong, G.D. Stucky, A. Thomas, Adv. Funct. Mater. 23 (2013) 3661–3667.
[16] M.K. Bhunia, K. Yamauchi, K. Takanabe, Angew. Chem. Int. Ed. Engl. 53 (2014) 11001–11005.
[17] G. Zhang, M. Zhang, X. Ye, X. Qiu, S. Lin, X. Wang, Adv. Mater. 26 (2014) 805–809.
[18] S. Hu, F. Li, Z. Fan, F. Wang, Y. Zhao, Z. Lv, Dalton Trans. 44 (2015) 1084–1092.
[19] H. Yan, Y. Chen, S. Xu, Int. J. Hydrogen Energy 37 (2012) 125–133.
[20] X. Lu, Q. Wang, D. Cui, J. Mater. Sci. Technol. 26 (2010) 925–930.
[21] Y. Zang, L. Li, Y. Zuo, H. Lin, G. Li, X. Guan, RSC Adv. 3 (2013) 13646–13650.
[22] W. Sundermeyer, Angew. Chem. Int. Ed. Engl. 4 (1965) 222–238.
[23] W. Sundermeyer, Chem. Unserer Zeit 1 (1967) 150.
[24] M.J. Bojdys, J.O. Muller, M. Antonietti, A. Thomas, Chemistry 14 (2008) 8177–8182.
[25] E. Wirnhier, M. Doblinger, D. Gunzelmann, J. Senker, B.V. Lotsch, W. Schnick, Chemistry 17 (2011) 3213–3221.
[26] K. Schwinghammer, B. Tuffy, M.B. Mesch, E. Wirnhier, C. Martineau, F. Taulelle, W. Schnick, J. Senker, B.V. Lotsch, Angew. Chem. Int. Ed. Engl. 52 (2013) 2435–2439.
[27] K. Schwinghammer, M.B. Mesch, V. Duppel, C. Ziegler, J. Senker, B.V. Lotsch, J. Am. Chem. Soc. 136 (2014) 1730–1733.
[28] Y. Zheng, L. Lin, B. Wang, X. Wang, Angew. Chem. Int. Ed. Engl. 54 (2015) 12868–12884.
[29] Y. Li, H. Xu, S. Ouyang, D. Lu, X. Wang, D. Wang, J. Ye, J. Mater. Chem. A 4 (2016) 2943–2950.
[30] X. Zhang, X. Xie, H. Wang, J. Zhang, B. Pan, Y. Xie, J. Am. Chem. Soc. 135 (2012) 18–21.
[31] J.J. Wang, Z.J. Li, X.B. Li, X.B. Fan, Q.Y. Meng, S. Yu, C.B. Li, J.X. Li, C.H. Tung, L.Z. Wu, ChemSusChem 7 (2014) 1468–1475.
[32] X.L. Wang, W.Q. Fang, H.F. Wang, H. Zhang, H. Zhao, Y. Yao, H.G. Yang, J. Mater. Chem. A 1 (2013) 14089–14096.
[33] C.L. Schmidt, M. Jansen, J. Mater. Chem. 20 (2010) 4183–4192.
[34] B. Yue, Q. Li, H. Iwai, T. Kako, J. Ye, Sci. Technol. Adv. Mater. 12 (2011) 034401.
[35] X. Wang, L. Wang, F. Zhao, C. Hu, Y. Zhao, Z. Zhang, S. Chen, G. Shi, L. Qu, Nanoscale 7 (2015) 3035–3042.
[36] Z. Zhang, J. Huang, Q. Yuan, B. Dong, Nanoscale 6 (2014) 9250–9256.
[37] H. Yu, R. Shi, Y. Zhao, T. Bian, Y. Zhao, C. Zhou, G.I.N. Waterhouse, L.Z. Wu, C.H. Tung, T. Zhang, Adv. Mater. 29 (2017) 1605148.
[38] Y. Wang, Y. Li, W. Ju, J. Wang, H. Yao, L. Zhang, J. Wang, Z. Li, Carbon 102 (2016) 477–486.
[39] A. Thomas, A. Fischer, F. Goettmann, M. Antonietti, J.-O. Müller, R. Schlögl, J.M. Carlsson, J. Mater. Chem. 18 (2008) 4893–4908.
[40] H. Lin, L. Ding, Z. Pei, Y. Zhou, J. Long, W. Deng, X. Wang, Appl. Catal. B: Environ. 160 (2014) 98–105.
[41] L. Jing, Y. Qu, B. Wang, S. Li, B. Jiang, L. Yang, W. Fu, H. Fu, J. Sun, Sol. Energy Mater. Sol. Cells 90 (2006) 1773–1787.
[42] H. Gao, S. Yan, J. Wang, Y.A. Huang, P. Wang, Z. Li, Z. Zou, Phys. Chem. Chem. Phys. 15 (2013) 18077–18084.
[43] M. Tabbal, T. Christidis, S. Isber, P. Mérel, M.A. El Khakani, M. Chaker, A. Amassian, L. Martinu, J. Appl. Phys. 98 (2005) 044310.
[44] J. Sun, J. Zhang, M. Zhang, M. Antonietti, X. Fu, X. Wang, Nat. Commun. (2012) 1139.
[45] L. Kong, Y. Dong, P. Jiang, G. Wang, H. Zhang, N. Zhao, J. Mater. Chem. A 4 (2016) 9998–10007.